Published in final edited form as:
Curr Biol. 2012 June 19; 22(12): 1109–1115. doi:10.1016/j.cub.2012.04.019.

Septin-driven Coordination of Actin and Microtubule Remodeling Regulates the Collateral Branching of Axons

Jianli Hu[1,2], **Xiaobo Bai**[1], **Jonathan R. Bowen**[1], **Lee Dolat**[1], **Farida Korobova**[3], **Wenqian Yu**[2], **Peter W. Baas**[2], **Tatyana Svitkina**[3], **Gianluca Gallo**[2,4], and **Elias T. Spiliotis**[1,2,4]

[1]Department of Biology, Drexel University, Philadelphia, PA 19104, USA

[2]Department of Neurobiology and Anatomy, Drexel University College of Medicine, Philadelphia, PA 19129, USA

[3]Department of Biology, University of Pennsylvania, Philadelphia, PA 19104, USA

Summary

Axon branching is fundamental to the development of the peripheral and central nervous system [1, 2]. Branches that sprout from the axon shaft are termed collateral or interstitial branches [3, 4]. Collateral branching of axons requires the formation of filopodia from actin microfilaments (F-actin) and their engorgement with microtubules (MTs) that splay from the axon shaft [4–6]. The mechanisms that drive and coordinate the remodeling of actin and MTs during branch morphogenesis are poorly understood. Septins comprise a family of GTP-binding proteins that oligomerize into higher order structures, which associate with membranes and the actin and microtubule cytoskeleton [7, 8]. Here, we show that collateral branching of axons requires SEPT6 and SEPT7, two interacting septins [9]. In the axons of sensory neurons, both SEPT6 and SEPT7 accumulate at incipient sites of filopodia formation. We show that SEPT6 localizes to axonal patches of F-actin and increases the recruitment of cortactin, a regulator of Arp2/3-mediated actin polymerization, triggering the emergence of filopodia. Conversely, SEPT7 promotes the entry of axonal MTs into filopodia, enabling the formation of collateral branches. Surprisingly, septins provide a novel mechanism for the collateral branching of axons by coordinating the remodeling of the actin and microtubule cytoskeleton.

Results

SEPT6 and SEPT7 Regulate Axon Collateral Branching

Dorsal root ganglia (DRG) neurons from chick embryos generate collateral branches *in vivo* and *in vitro* [10, 11]. Using this model system, we focused our studies on septins 6 and 7, which have been separately shown to be required for the morphogenesis of dendrites [12–14], but their molecular functions remain unknown. To determine whether SEPT6 and SEPT7 constitute a hetero-oligomeric complex, we performed quantitative

Correspondence: Elias T. Spiliotis, Department of Biology, Drexel University, PISB 423, 3245 Chestnut St, Philadelphia, PA 19104, Tel: 215-571-3552, Fax: 215-895-1273, ets33@drexel.edu. Gianluca Gallo, Department of Neurobiology & Anatomy, Drexel University College of Medicine, 2900 Queen Lane, Philadelphia, PA 19129, Tel: 215-991-8288, Fax: 215-843-0980, GGallo@drexelmed.edu.
[4]These authors contributed equally to this work

immunoprecipitations and immunodepletions. Approximately 24% of total SEPT6 precipitated with SEPT7 (Figure S1A–B), and immunodepletion of SEPT6 to ~70% of its total levels led to ~30% depletion of SEPT7 (Figure S1C). Thus, a fraction of SEPT6 (~24%) and SEPT7 (~43%) appear to interact with one another, indicating that these septins could have overlapping and distinct functions.

To test whether septins are involved in axon collateral branching, we over-expressed and depleted SEPT6 and SEPT7. Over-expression of SEPT6-GFP and SEPT7-GFP in embryonic day 10 (E10) DRGs resulted in a 2–3-fold increase in the number of branches per 50 μm of distal axon length (Figure 1A–D). The percentage of axons with 2 or more branches also increased (Figure 1E); the branches of control and septin over-expressing axons contained the synaptic vesicle marker synaptotagmin 1 and thus, appeared to be functional (Figure S2A–C). Septin over-expression also increased axon branching in primary rat hippocampal neurons (Figure S2D–H). Next we transfected E7 DRGs with GFP-expressing pSUPER plasmids that expressed chicken-specific SEPT6 and SEPT7 shRNAs. We chose E7 DRGs because they generate more branches and thus, allow for quantifiable effects after 2–3 days of septin knockdown. This approach led to ~50% depletion of endogenous septins (Figure S2I–P). SEPT6- and SEPT7-depleted neurons developed 3-times less collateral branches than control cells, and the percentage of axons with no branches increased (Figure 1F–J). The phenotype was rescued by expression of shRNA-resistant SEPT6-GFP and SEPT7-GFP (Figure 1I–J). Consistent with previous reports [15, 16], septin depletion also decreased the length of axons, but next we focused on the mechanisms of axon branching, which are more similar to axon guidance than extension [5, 6].

SEPT6 and SEPT7 at Sites of Filopodia Formation – SEPT6 Regulates the Rate of Filopodial Initiation

We sought to determine the spatiotemporal distribution of SEPT6 and SEPT7 with respect to axonal filopodia, which are the precursors of collateral branches [4]. In DRG axons, SEPT6 displayed a punctate distribution throughout the axon shaft and accumulated at the base of F-actin-rich filopodia (Figure 2A). SEPT7 was less punctate than SEPT6 in the axonal shaft and localized to chevron-like structures at the base of filopodia (Figure 2B–C). Simultaneous staining for SEPT6 and SEPT7 showed a distinct pattern of localization with some overlap at the neck of filopodial protrusions (Figure 2C; inset arrow). Time-lapse imaging of live neurons with low levels of SEPT6-GFP and SEPT7-GFP expression revealed that both septins accumulate at incipient sites of filopodia formation (Figure 2D–E, Movies S1–2). These data suggest that SEPT6 and SEPT7 could play a critical role in the formation of axonal filopodia.

We tested this hypothesis by measuring the rate of filopodia formation in live DRGs after septin over-expression and depletion. Over-expression of SEPT6-GFP doubled the rate of filopodia formation, but SEPT7-GFP did not have an effect (Figure 2F, Movie S3). Similarly, expression of SEPT6 shRNA, but not SEPT7 shRNA, decreased the rate of filopodia formation (Figure 2G). Thus, SEPT6 functions at the level of filopodial initiation, while SEPT7 does not appear to have a role in this process.

SEPT6 Increases Cortactin Recruitment to Axonal Patches of F-actin and Triggers Emergence of Filopodia

Because axonal filopodia emerge from patches of F-actin [17–19], we probed for the localization and function of SEPT6 with respect to actin patches. SEPT6 colocalized with F-actin in axonal patches (Figure 3A, see also arrowheads in Figure 2A) and at the base of axonal filopodia (Figure 3A). In contrast, SEPT7 localized to the sides of F-actin patches and the neck of filopodia, exhibiting little overlap with actin patches (Figure 3B). These data

indicated that SEPT6 could bind preferentially to Arp2/3-nucleated branched actin filaments, which are prevalent in actin patches and at the base of axonal filopodia [19]. Indeed, *in vitro* binding of recombinant SEPT6-GFP to actin filaments and branch points increased in the presence of Arp2/3 (Figure S3A–D), while SEPT7-GFP binding was independent of actin branching and occurred predominately along the length of actin filaments (Figure S3E–H). Consistent with these results, a recent yeast two-hybrid screen identified Arp2 as an interacting partner of SEPT6, but not SEPT7 [20]. Thus, SEPT6 appears to associate preferentially with the Arp2/3-dependent patches of F-actin.

Although the majority of filopodia emerge from actin patches, only a fraction of patches develops to filopodia [17–19]. In time-lapse movies of mCherry-actin and SEPT6-GFP, actin patches formed and dissipated together with SEPT6 (Figure 3C). We therefore reasoned that SEPT6 could regulate the formation or lifespan of F-actin patches, and/or their conversion to axonal filopodia. Tracking and quantitative analysis of mCherry-actin showed that neither the over-expression nor depletion of SEPT6 affected the rate of formation and lifespan of F-actin patches (Figure S3I–L). Notably, though, SEPT6-GFP over-expression induced a two-fold increase in the percentage of actin patches that gave rise to filopodia (Figure 3D), and depletion of endogenous SEPT6 had the opposite effect (Figure 3E). Over-expression or depletion of SEPT7 did not affect any of the parameters of mCherry-actin patch dynamics (Figure 3D–E and Figure S3I–L). Therefore, SEPT6 appears to trigger the initiation of filopodia from F-actin patches.

To determine how SEPT6 promotes filopodia formation, we tested whether SEPT6 affects the localization of cortactin, an activator of Arp2/3-mediated actin polymerization, which has been shown to induce the protrusive activity of neuronal actin patches [19, 21]. SEPT6 and cortactin colocalized in actin patches and at the base of filopodia (Figure 3F–G). Over-expression and depletion of SEPT6 increased and decreased the levels of cortactin in actin patches, respectively (Figure 3H–I). This effect was specific to cortactin, as the levels of the Wiskott-Aldrich syndrome related protein WAVE3 did not change (Figure S3M). Interestingly, SEPT6 over-expression also raised cortactin levels at the lamellipodia of epithelial cells (Figure S3N–O), suggesting that SEPT6-mediated recruitment of cortactin is a conserved mechanism for the induction of actin-based membrane protrusions from neurons to epithelia.

SEPT7 Promotes Entry of Axonal MTs into Filopodia

Formation of F-actin-rich filopodia is necessary but not sufficient for the morphogenesis of collateral branches, which must be invaded by axonal MTs in order to mature [22, 23]. Although SEPT7 does not function in the protrusive step of branch morphogenesis (Figure 2F–G), SEPT7 is clearly required for branch formation (Figure 1I–J). We therefore asked whether SEPT7 regulates the organization of axonal MTs during branching.

We over-expressed and depleted SEPT7 or SEPT6, and screened for the presence of MTs in axonal filopodia. In SEPT7-GFP-expressing axons, there were twice as many filopodia with MTs as in GFP- and SEPT6-GFP-expressing neurons (Figure 4A). In contrast, SEPT6-GFP over-expression did not increase MT presence in filopodia (Figure 4A). Depletion of endogenous SEPT6 or SEPT7, however, decreased MT-positive filopodia by 50% relative to controls (Figure 4B). Thus, both SEPT6 and SEPT7 are necessary, but only SEPT7 can promote MT localization in axonal filopodia. In agreement with this result, recombinant SEPT7-GFP bound *in vitro* to MTs directly and much stronger than SEPT6-GFP (Figure 4D–H).

Unbundling and fragmentation of the axonal bundle of MTs generate new MT plus ends and shorter MTs, which are free to enter into axonal filopodia [22, 23]. By staining for the MT

end binding protein EB1, we found that SEPT7-GFP over-expressing axons contained more MT plus ends than GFP- and SEPT6-GFP-expressing axons (Figure 4C). In SEPT7-GFP over-expressing axons, EB1 particles were seen in larger clusters and many of them colocalized with SEPT7-GFP (Figure S4A–B). In addition to this increase in MT ends, the axonal MT array appeared to unravel at sites of SEPT7-GFP accumulation (Figure 4J). In contrast, the axonal MT array in SEPT6-GFP-overexpressing axons was firmly bundled (Figure 4I). To confirm that the axonal cytoskeleton was indeed altered in SEPT7-GFP over-expressing DRGs, we used correlative fluorescence and platinum replica electron microscopy. At the nanometer scale of this imaging technique, axonal bundles appeared to split apart at sites of SEPT7-GFP accumulation, and individual cytoskeletal filaments were seen to stick out of the main axon shaft (Figure 4K and Figure S4C–E). Taken together, these data indicate that SEPT7 alters the organization of the main axon bundle, allowing MTs to enter nascent filopodia, which in turn mature to collateral branches.

Discussion

Septins have been shown to be essential for neuronal migration [16] and axon guidance [15], but the molecular function of septins was unknown. Here, we have shown that two interacting septins, SEPT6 and SEPT7, trigger actin and MT reorganization. Our results suggest that the combined action of SEPT6 and SEPT7 provides a coordinating mechanism for the collateral branching of axons.

Previous work has linked septins and actin organization to common signaling pathways [24, 25], but it was unknown if septins function in the assembly of F-actin structures [26]. Surprisingly, we have discovered that SEPT6 triggers the growth of F-actin patches into axonal filopodia. Because SEPT6 does not affect the formation or lifespan of actin patches, we posit that SEPT6 associates with actin patch filaments and F-actin branch points, and acts as a scaffold that increases the local concentration of cortactin, triggering the transition of actin patches to filopodia [21]. This scaffold-like function of SEPT6 resembles the role of SEPT2 as a scaffold of myosin II [27], and appears to be conserved in the lamellipodia of epithelial cells. Taken together, these results have uncovered an unexpected link between SEPT6 and Arp2/3-mediated actin polymerization.

SEPT7 alters the organization of axonal MTs, promoting their localization in filopodia. Previous work has shown that septins prevent microtubule-associated proteins (MAPs) from binding to MTs [25, 28]. Thus, it is possible that SEPT7 displaces neuronal MAPs, which protect axonal MTs from severing enzymes, resulting in the formation of new MT tips [29, 30]. Alternatively, SEPT7 may achieve the same effect by altering the post-translational modifications of MTs [25, 28]. The localization of SEPT7 to the base of axonal filopodia is similar to that observed at the base of dendritic spines [12, 13], suggesting that SEPT7 may also be involved in MT targeting to dendritic protrusions [31]. This role of SEPT7 would not preclude its putative function as a membrane diffusion barrier [32].

Although SEPT6 and SEPT7 perform distinct functions, a functional and physical crosstalk appears to be in effect. First, SEPT7 is functionally dependent on SEPT6; even though not in itself sufficient, SEPT6 is necessary for MT presence in filopodia (Figure 4A–B). Second, a significant fraction of SEPT6 and SEPT7 interact with one another (Figure S1). Third, some overlap in SEPT6 and SEPT7 localization is observed at the base of axonal filopodia (Figure 2). Taken together, our results suggest that SEPT6 and SEPT7 comprise a regulatory module, which activates the reorganization of the actin and MT cytoskeleton in a coordinated fashion, affecting the development of axon collateral branches. Future studies could exploit this role of septins to control the sprouting of axons after injury of the nervous system.

Supplementary Material

Refer to Web version on PubMed Central for supplementary material.

Acknowledgments

We thank Drs Roberto Dominguez and Suk Namgoonk (University of Pennsylvania), Makoto Kinoshita (Nagoya University) and Helge Ewers (ETH Zurich) for reagents. The work was supported by NIH grants GM097664 to ETS (PI), NS048090 to GG (PI), GM70898 to TS, NS028785 to PWB, a Drexel CURE grant to GG (PI) and ETS (Co-I), and NSF grant 0841245 to PWB.

References

1. O'Leary DD, Koester SE. Development of projection neuron types, axon pathways, and patterned connections of the mammalian cortex. Neuron. 1993; 10:991–1006. [PubMed: 8318235]
2. Schmidt H, Rathjen FG. Signalling mechanisms regulating axonal branching in vivo. Bioessays. 2010; 32:977–985. [PubMed: 20827677]
3. Gibson DA, Ma L. Developmental regulation of axon branching in the vertebrate nervous system. Development. 2011; 138:183–195. [PubMed: 21177340]
4. Gallo G. The cytoskeletal and signaling mechanisms of axon collateral branching. Dev Neurobiol. 2011; 71:201–220. [PubMed: 21308993]
5. Dent EW, Tang F, Kalil K. Axon guidance by growth cones and branches: common cytoskeletal and signaling mechanisms. Neuroscientist. 2003; 9:343–353. [PubMed: 14580119]
6. Kornack DR, Giger RJ. Probing microtubule +TIPs: regulation of axon branching. Curr Opin Neurobiol. 2005; 15:58–66. [PubMed: 15721745]
7. Weirich CS, Erzberger JP, Barral Y. The septin family of GTPases: architecture and dynamics. Nat Rev Mol Cell Biol. 2008; 9:478–489. [PubMed: 18478031]
8. Spiliotis, ET.; Nelson, WJ. Septin functions in the mammalian cytoskeleton. In: Hall, PA.; Russell, SEH.; Pringle, JR., editors. The Septins. Chichester: John Wiley and Sons; 2008. p. 229-246.
9. Sheffield PJ, Oliver CJ, Kremer BE, Sheng S, Shao Z, Macara IG. Borg/septin interactions and the assembly of mammalian septin heterodimers, trimers, and filaments. J Biol Chem. 2003; 278:3483–3488. [PubMed: 12446710]
10. Davis BM, Frank E, Johnson FA, Scott SA. Development of central projections of lumbosacral sensory neurons in the chick. J Comp Neurol. 1989; 279:556–566. [PubMed: 2918087]
11. Letourneau PC. Analysis of microtubule number and length in cytoskeletons of cultured chick sensory neurons. J Neurosci. 1982; 2:806–814. [PubMed: 7086485]
12. Xie Y, Vessey JP, Konecna A, Dahm R, Macchi P, Kiebler MA. The GTP-binding protein Septin 7 is critical for dendrite branching and dendritic-spine morphology. Curr Biol. 2007; 17:1746–1751. [PubMed: 17935997]
13. Tada T, Simonetta A, Batterton M, Kinoshita M, Edbauer D, Sheng M. Role of Septin cytoskeleton in spine morphogenesis and dendrite development in neurons. Curr Biol. 2007; 17:1752–1758. [PubMed: 17935993]
14. Cho SJ, Lee H, Dutta S, Song J, Walikonis R, Moon IS. Septin 6 regulates the cytoarchitecture of neurons through localization at dendritic branch points and bases of protrusions. Mol Cells. 2011; 32:89–98. [PubMed: 21544625]
15. Finger FP, Kopish KR, White JG. A role for septins in cellular and axonal migration in C. elegans. Dev Biol. 2003; 261:220–234. [PubMed: 12941631]
16. Shinoda T, Ito H, Sudo K, Iwamoto I, Morishita R, Nagata K. Septin 14 is involved in cortical neuronal migration via interaction with Septin 4. Mol Biol Cell. 2010; 21:1324–1334. [PubMed: 20181826]
17. Ketschek A, Spillane M, Gallo G. Mechanism of NGF-induced formation of axonal filopodia: NGF turns up the volume, but the song remains the same? Commun Integr Biol. 2011; 4:55–58. [PubMed: 21509179]

18. Loudon RP, Silver LD, Yee HF Jr, Gallo G. RhoA-kinase and myosin II are required for the maintenance of growth cone polarity and guidance by nerve growth factor. J Neurobiol. 2006; 66:847–867. [PubMed: 16673385]
19. Spillane M, Ketschek A, Jones SL, Korobova F, Marsick B, Lanier L, Svitkina T, Gallo G. The actin nucleating Arp2/3 complex contributes to the formation of axonal filopodia and branches through the regulation of actin patch precursors to filopodia. Dev Neurobiol. 2011; 71:747–758. [PubMed: 21557512]
20. Nakahira M, Macedo JN, Seraphim TV, Cavalcante N, Souza TA, Damalio JC, Reyes LF, Assmann EM, Alborghetti MR, Garratt RC, et al. A draft of the human septin interactome. PLoS One. 2010; 5:e13799. [PubMed: 21082023]
21. Mingorance-Le Meur A, O'Connor TP. Neurite consolidation is an active process requiring constant repression of protrusive activity. EMBO J. 2009; 28:248–260. [PubMed: 19096364]
22. Dent EW, Callaway JL, Szebenyi G, Baas PW, Kalil K. Reorganization and movement of microtubules in axonal growth cones and developing interstitial branches. J Neurosci. 1999; 19:8894–8908. [PubMed: 10516309]
23. Yu W, Ahmad FJ, Baas PW. Microtubule fragmentation and partitioning in the axon during collateral branch formation. J Neurosci. 1994; 14:5872–5884. [PubMed: 7931550]
24. Ito H, Iwamoto I, Morishita R, Nozawa Y, Narumiya S, Asano T, Nagata K. Possible role of Rho/Rhotekin signaling in mammalian septin organization. Oncogene. 2005; 24:7064–7072. [PubMed: 16007136]
25. Kremer BE, Haystead T, Macara IG. Mammalian septins regulate microtubule stability through interaction with the microtubule-binding protein MAP4. Mol Biol Cell. 2005; 16:4648–4659. [PubMed: 16093351]
26. Kinoshita M, Field CM, Coughlin ML, Straight AF, Mitchison TJ. Self- and actin-templated assembly of Mammalian septins. Dev Cell. 2002; 3:791–802. [PubMed: 12479805]
27. Joo E, Surka MC, Trimble WS. Mammalian SEPT2 is required for scaffolding nonmuscle myosin II and its kinases. Dev Cell. 2007; 13:677–690. [PubMed: 17981136]
28. Spiliotis ET, Hunt SJ, Hu Q, Kinoshita M, Nelson WJ. Epithelial polarity requires septin coupling of vesicle transport to polyglutamylated microtubules. J Cell Biol. 2008; 180:295–303. [PubMed: 18209106]
29. Qiang L, Yu W, Andreadis A, Luo M, Baas PW. Tau protects microtubules in the axon from severing by katanin. J Neurosci. 2006; 26:3120–3129. [PubMed: 16554463]
30. Yu W, Qiang L, Solowska JM, Karabay A, Korulu S, Baas PW. The microtubule-severing proteins spastin and katanin participate differently in the formation of axonal branches. Mol Biol Cell. 2008; 19:1485–1498. [PubMed: 18234839]
31. Hu X, Viesselmann C, Nam S, Merriam E, Dent EW. Activity-dependent dynamic microtubule invasion of dendritic spines. J Neurosci. 2008; 28:13094–13105. [PubMed: 19052200]
32. Barral Y, Mansuy IM. Septins: cellular and functional barriers of neuronal activity. Curr Biol. 2007; 17:R961–963. [PubMed: 18029249]

Highlights

- Collateral branching of axons is regulated by SEPT6 and SEPT7
- SEPT6 and SEPT7 are recruited to nascent sites of filopodia formation
- SEPT6 recruits cortactin to patches of F-actin and triggers filopodia formation
- SEPT7 alters axonal MT organization, triggering MT entry into filopodia

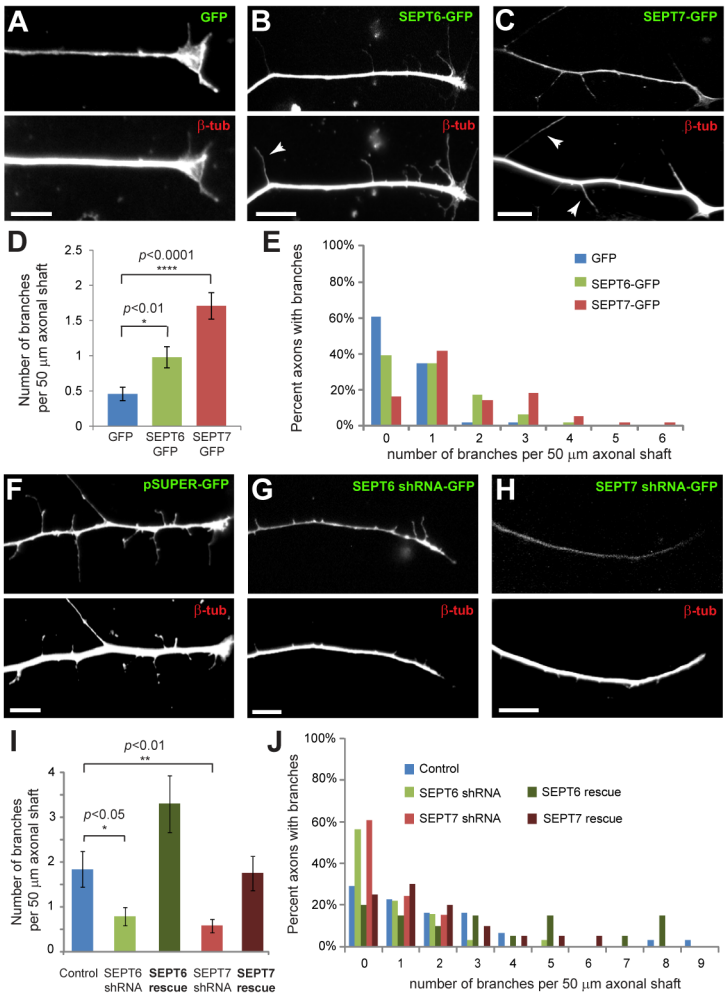

Figure 1. SEPT6 and SEPT7 Regulate the Collateral Branching of Sensory Axons

(A–C) Distal axon segments of E10 DRGs transfected with GFP, SEPT6-GFP and SEPT7-GFP and stained for β-tubulin. Arrowheads point to collateral branches. Scale bars: ~10 μm. (D–E) Graph shows the mean number of >5 μm-long branches per 50 μm of distal axon shaft in DRGs transfected with GFP (N=46), SEPT6-GFP (N=46) and SEPT7-GFP (N=55). Histogram (E) shows percentage of axon segments with 0–6 branches. (F–H) Distal axon segments of E7 DRGs transfected with pSUPER-GFP plasmids expressing SEPT6 and SEPT7 shRNAs and stained for β-tubulin. Scale bars: ~10 μm. (I–J) Graph shows the mean number of >5 μm-long branches per 50 μm of distal axon shaft in DRGs transfected with control pSUPER-GFP (N=31), shRNAs against SEPT6 (N=32) and SEPT7 (N=33), and rescue plasmids encoding for shRNA-resistant SEPT6 (N=20) and SEPT7 (N=20). Histogram (J) shows percentage of axon segments with 0–9 branches.

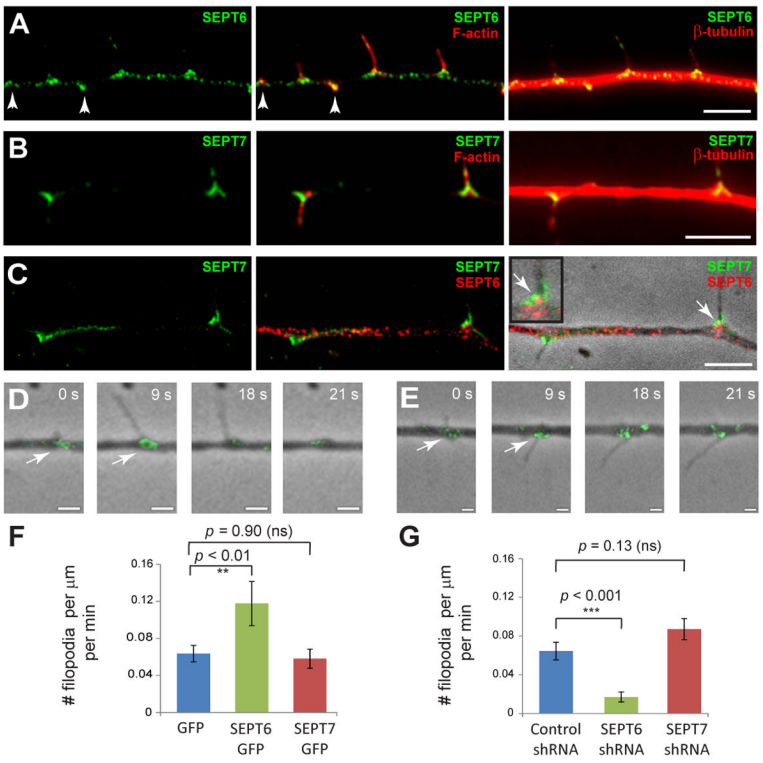

Figure 2. SEPT6 and SEPT7 Localize to the Base of Axonal Filopodia - SEPT6 Controls Rate of Filopodia Formation

(A–C) E10 DRG neurons were fixed and stained with Cy3-conjugated anti-β-tubulin and rabbit antibodies against SEPT6 (A) or SEPT7 (B) followed by secondary staining with Alexa 647-phalloidin and DyLight 488 anti-rabbit IgG. Staining for both SEPT6 and SEPT7 (C) was performed with anti-SEPT7, FITC-conjugated monovalent anti-IgG and anti-SEPT6 conjugated to Alexa 555. Arrowheads point to patches of F-actin. Arrow points to a region of overlap between SEPT6 and SEPT7. Scale bars: ~5 μm. (D–E) Still frames from time-lapse microscopy of DRG axons expressing SEPT6-GFP (D, Movie S1) and SEPT7-GFP (E, Movie S2). In panel D, frame 0 corresponds to frame 3 (9 s) of Movie S1. Arrows point to SEPT6-GFP and SEPT7-GFP accumulating at the base of nascent filopodia. Note that the GFP-tagged probes are expressed at the lowest detectable levels and thus do not precisely mirror the distribution of endogenous septins. Scale bars: ~1 μm. (F–G) Graphs show mean number of filopodia formed per minute per μm of axon in live DRGs transfected with GFP (N=19), SEPT6-GFP (N=24) and SEPT7-GFP (N=19) or with control pSUPER-GFP (N=16) and shRNAs against SEPT6 (N=15) and SEPT7 (N=19).

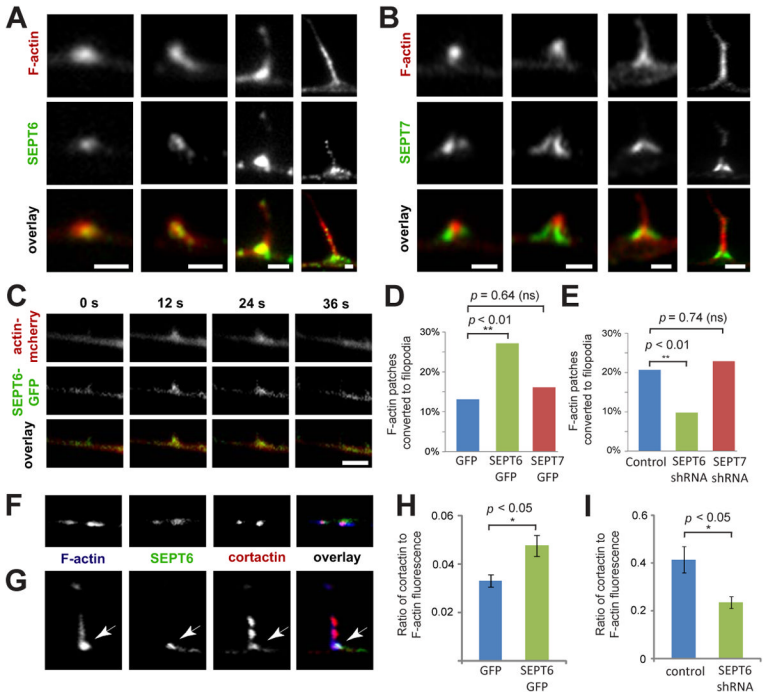

Figure 3. SEPT6 Increases Cortactin Recruitment to F-actin Patches, Triggering the Formation of Axonal Filopodia

(A–B) Galleries show high magnification images of F-actin patches and filopodia in E10 DRG axons stained for SEPT6 and SEPT7. Scale bars: ~1 μm. (C) Still frames from time-lapse fluorescence microscopy of SEPT6-GFP and mCherry-actin in a DRG axon. Scale bar: ~ 2 μm. (D–E) Graphs show percentage of mCherry-actin patches converted to filopodia in live DRG neurons transfected with GFP (N=99), SEPT6-GFP (N=227) and SEPT7-GFP (N=155) or control pSUPER-GFP (N=208) and shRNAs against SEPT6 (N=163) and SEPT7 (N=118). (F–G) Confocal microscopy images of F-actin patches (F) and a filopodium (G) stained for SEPT6 and cortactin in E10 DRG axons. Arrow points to colocalization of SEPT6 and cortactin at the base of the filopodium. Scale bars: ~1 μm. (H–I) Graphs show the mean ratio of cortactin to F-actin fluorescence intensity in actin patches of DRG neurons transfected with GFP (N=85 patches; 23 axons) and SEPT6-GFP (N=107 patches; 23 axons) or control pSUPER-GFP (N=53 patches; 18 axons) and shRNA against SEPT6 (N=52 patches; 13 axons).

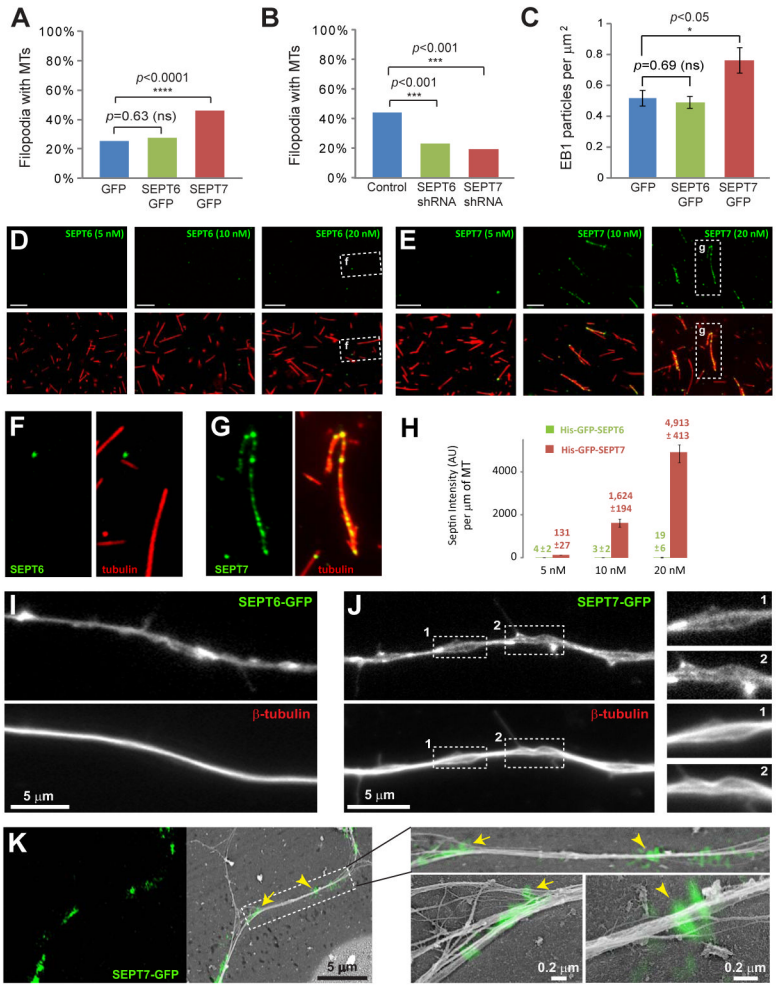

Figure 4. SEPT7 Alters Axonal MT Organization, Facilitating MT Entry into Filopodia

(A–B) Graphs show percentage of filopodia containing MTs in DRG neurons transfected with GFP (N=215; 46 cells), SEPT6-GFP (N=383; 48 cells) and SEPT7-GFP (N=460; 55 cells) or pSUPER-GFP (N=290; 31 cells) and shRNAs against SEPT6 (N=191; 32 cells) and SEPT7 (N=215; 35 cells). (C) Graph shows number of EB1 particles per μm^2 of axon surface in DRG neurons transfected with GFP (N=15), SEPT6-GFP (N=19) and SEPT7-GFP (N=18). (D–H) Images show rhodamine-labeled MTs (red) coated with increasing concentrations of His-GFP-tagged SEPT6 and SEPT7 (green). Individual MTs are outlined and shown in higher magnification. Graph shows total fluorescence intensity of GFP per MT length (N=52–57). (I–J) Images show β-tubulin-stained DRG neurons that over-express SEPT6-GFP and SEPT7-GFP. Insets show areas of axonal MT unraveling in higher magnification. (F) Correlative fluorescence and platinum replica EM images of DRG neurons over-expressing SEPT7-GFP (green). Arrow and arrowhead point to sites of SEPT7-GFP accumulation shown in higher magnification.